



University  
of Glasgow

Labrosse, N. and Gouttebroze, P. and Vial, J.-C. (2006) *The helium spectrum in moving solar prominences*. In: Lacoste, H. (ed.) Proceedings of SOHO-17 10 years of SOHO and Beyond 7 - 12 May 2006, Giardini Naxos, Sicily, Italy. ESA Special Publication (617). ESA Publications Division, Noordwijk, The Netherlands. ISBN 9789290929284

<http://eprints.gla.ac.uk/24808/>

Deposited on: 28 January 2010

# THE HELIUM SPECTRUM IN MOVING SOLAR PROMINENCES

N. Labrosse<sup>1</sup>, P. Gouttebroze<sup>2</sup>, and J.-C. Vial<sup>2</sup>

<sup>1</sup>*Institute of Mathematical and Physical Sciences, University of Wales Aberystwyth, Ceredigion SY23 3BZ, UK, Email: nll@aber.ac.uk*

<sup>2</sup>*Institut d'Astrophysique Spatiale, CNRS/Université Paris Sud, 91405 Orsay cedex, France, Email: pierre.gouttebroze@ias.u-psud.fr, jean-claude.vial@ias.u-psud.fr*

## ABSTRACT

We present the first computations of helium line profiles emitted by a moving prominence. The effect of Doppler dimming is investigated on the line profiles and emergent intensities of the EUV resonance lines of He I at 584 Å and 537 Å and He II at 304 Å. We also study the effect of frequency redistribution in the line formation mechanisms.

## 1. MODELLING OF AN ERUPTIVE PROMINENCE

We follow the approach of Gontikakis et al. (1997a,b) who computed the hydrogen spectrum emitted by an eruptive prominence. We use our non local thermodynamic equilibrium radiative transfer code where the prominence is modelled as a plane-parallel slab standing vertically above the solar surface and moving upward as a solid body. We only consider isothermal and isobaric prominence models. The numerical procedure has been described in Labrosse & Gouttebroze (2001, 2004) and we sum it up as follows: 1) Equations for pressure equilibrium, ionisation and statistical equilibria of the hydrogen atom are solved, together with the radiative transfer for the hydrogen lines and continuum. 2) Statistical equilibrium and radiative transfer equations are solved for the other elements (here, He I and He II).

The incident radiation is represented by the mean intensity:

$$J_0(\nu) = \frac{1}{4\pi} \oint I_0 \left( \nu + \frac{\nu_0}{c} \mathbf{V} \cdot \mathbf{n}', \mathbf{n}' \right) d\mathbf{n}', \quad (1)$$

with  $I_0(\nu, \mathbf{n})$  the specific intensity of the incident radiation,  $\mathbf{n}'$  the direction of the incident photon, and  $\mathbf{V}$  the radial velocity.  $J_0(\nu)$  is calculated at a given height, taking into account the center-to-limb variations of the incident radiation.

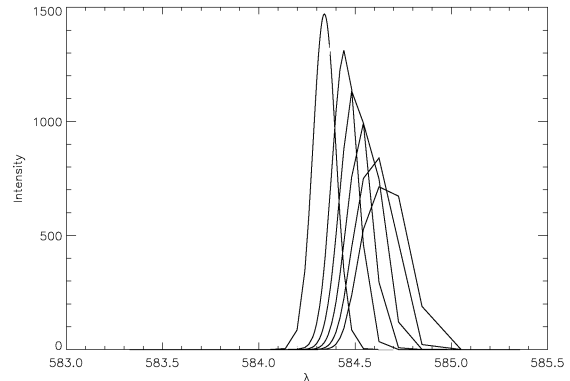


Figure 1. Angle-averaged incident profiles in the He I 584 line for a prominence located at 50000 km above the limb, and for velocities ranging from 0 (black curve) to 240 km s<sup>-1</sup> (step=40 km s<sup>-1</sup>). The incident profile is shifted towards the red when the velocity increases. Intensity in erg s<sup>-1</sup> cm<sup>-2</sup> sr<sup>-1</sup> Å<sup>-1</sup>.

Fig. 1 shows that the Doppler effect induces a shift of the incident profile, and the variation of the Doppler shift with direction induces a distortion of the incident profile. As the velocity increases, the maximum of the absorption profile of a line is moved towards the blue wing of the incident profile.

## 2. FREQUENCY REDISTRIBUTION

In solar prominences, the redistribution in frequency during the scattering of the incident radiation in resonance lines is best described by a combination of complete frequency redistribution (CRD) and coherent scattering. This leads us to use the standard partial redistribution (PRD) approximation to treat the scattering of the incident radiation. We compare two cases: in the CRD case, all helium lines are treated in CRD, while in the PRD case, we consider PRD for the resonance lines He I  $\lambda\lambda$  584 and 537 Å and He II  $\lambda$  304 Å lines. The prominence parameters are T=6500 K, p=0.1 dyn cm<sup>-2</sup>,

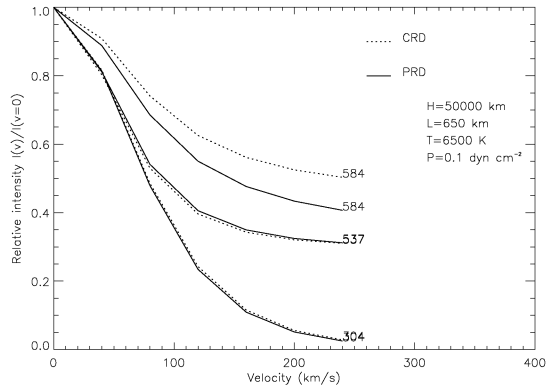


Figure 2. Integrated intensities in CRD (dotted line) and PRD (solid line). The thermodynamic parameters (height, width, temperature, pressure) of the prominence are shown on the figure.

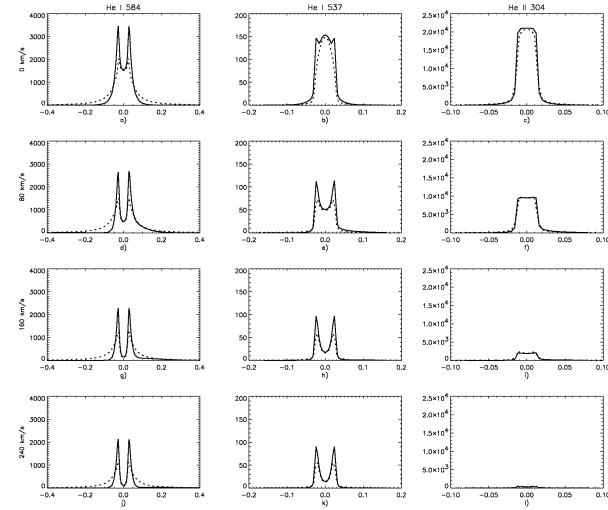


Figure 3. Line profiles in CRD (dotted line) and PRD (solid line). Same model as in Fig. 2.

$L=650$  km, and  $H=50000$  km. Fig. 2 shows that for this particular prominence model, the effect of frequency redistribution is especially important for the first resonance line of He I at  $584 \text{ \AA}$ . For the other two lines, CRD and PRD lead to similar relative intensities at all velocities. Fig. 3 shows that the line profiles differ between the CRD and PRD case. Therefore, it is important to compute the helium spectrum in PRD if we want to compare the calculations with observations.

### 3. SENSITIVITY TO TEMPERATURE

We compute several prominence models at two different temperatures (8000 K and 15000 K) for velocities between 0 and  $400 \text{ km s}^{-1}$ , keeping other parameters fixed, and using PRD. Fig. 4 shows that there is little difference between the two temperatures for the relative intensity of

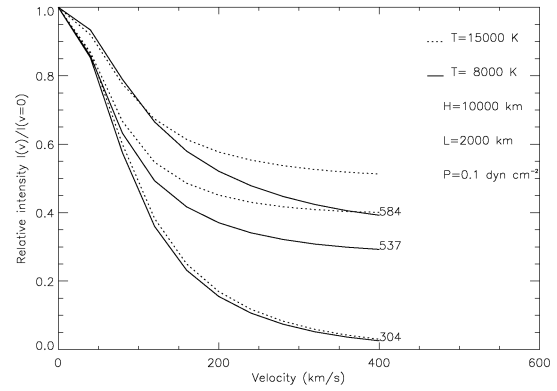


Figure 4. Relative intensity as a function of velocity at 8000 K and 15000 K for He I  $\lambda\lambda 584$  and  $537 \text{ \AA}$  and He II  $\lambda 304 \text{ \AA}$ .

the He II line, which is indeed mainly formed by resonant scattering of the incident radiation (Labrosse & Gouttebroze, 2001). The He I resonance lines show some sensitivity to the temperature: at high temperatures, the collisional excitation becomes non negligible for these lines. For each He I resonance line, the difference between the cold and hot prominence is more evident as the velocity increases. The contribution of resonant scattering for the line formation decreases with increasing velocity. For all lines, at velocities greater than  $150 \text{ km s}^{-1}$ , the relative intensity at 15000 K is greater than the relative intensity at 8000 K, and the relative emergent intensities are less dependent on the velocity. More diagnostic can be done using the line profiles, as illustrated with Figs. 5 and 6.

**He I  $\lambda 584 \text{ \AA}$  and He I  $\lambda 537 \text{ \AA}$  lines:** for all non-zero velocities, the incident profile, which is a single-peak emission line (see Fig. 1), is quasi-coherently scattered in the red wing of the line. At low temperature and low speeds, we see some asymmetry in the line profile, with some intensity enhancement in the red part. This asymmetry still exists at high speeds but is smaller. For both temperatures the reversal at line centre is more pronounced with increasing velocity. At high temperature, the asymmetry in the line profile is less pronounced than at low temperature. At a given temperature, the red wing of the profile first increases, and then decreases, with velocity.

**He II  $\lambda 304 \text{ \AA}$  line:** under the physical conditions considered in this study, its intensity is mainly dependent on the incident radiation. At a given speed, the intensity at line centre is the same for both temperatures. The only difference is that the profiles are broader at 15000 K than at 8000 K.

### 4. CONCLUSIONS

Partial redistribution in frequency is necessary to compute the profiles of the helium resonance lines emitted

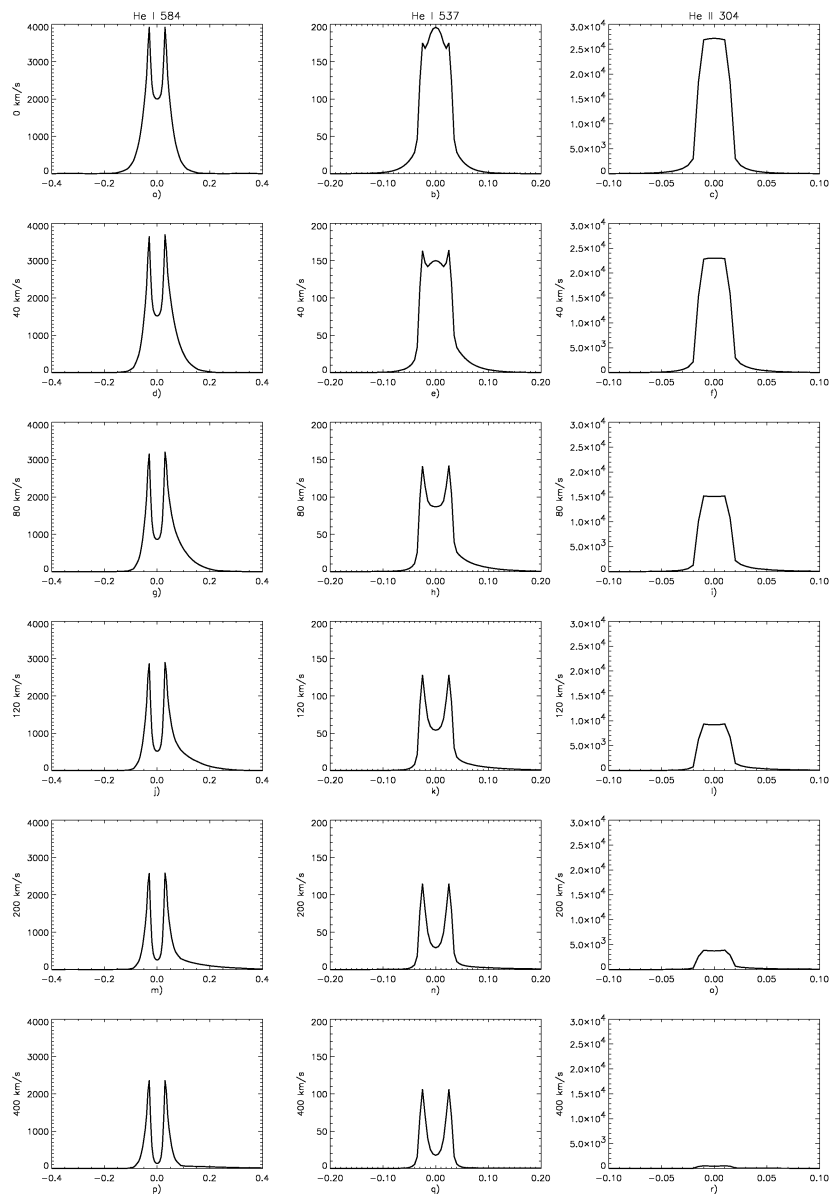


Figure 5. Line profiles for  $T=8000$  K,  $p=0.1$  dyn  $cm^{-2}$ ,  $L=2000$  km. Abscissa is  $\Delta\lambda$  in  $\text{\AA}$ .

by moving material in prominences. Velocity effects are more visible when thermal emission is low. Combining Doppler dimming / brightening effects on hydrogen and helium lines with the apparent motion of the prominence material brought by SOHO or future imagers (e.g. SOLAR-B, STEREO), the full velocity vector can be inferred.

Labrosse, N. & Gouttebroze, P. 2004, ApJ, 617, 614

## REFERENCES

- Gontikakis, C., Vial, J.-C., & Gouttebroze, P. 1997a, A&A, 325, 803  
 Gontikakis, C., Vial, J.-C., & Gouttebroze, P. 1997b, Sol. Phys., 172, 189  
 Labrosse, N. & Gouttebroze, P. 2001, A&A, 380, 323

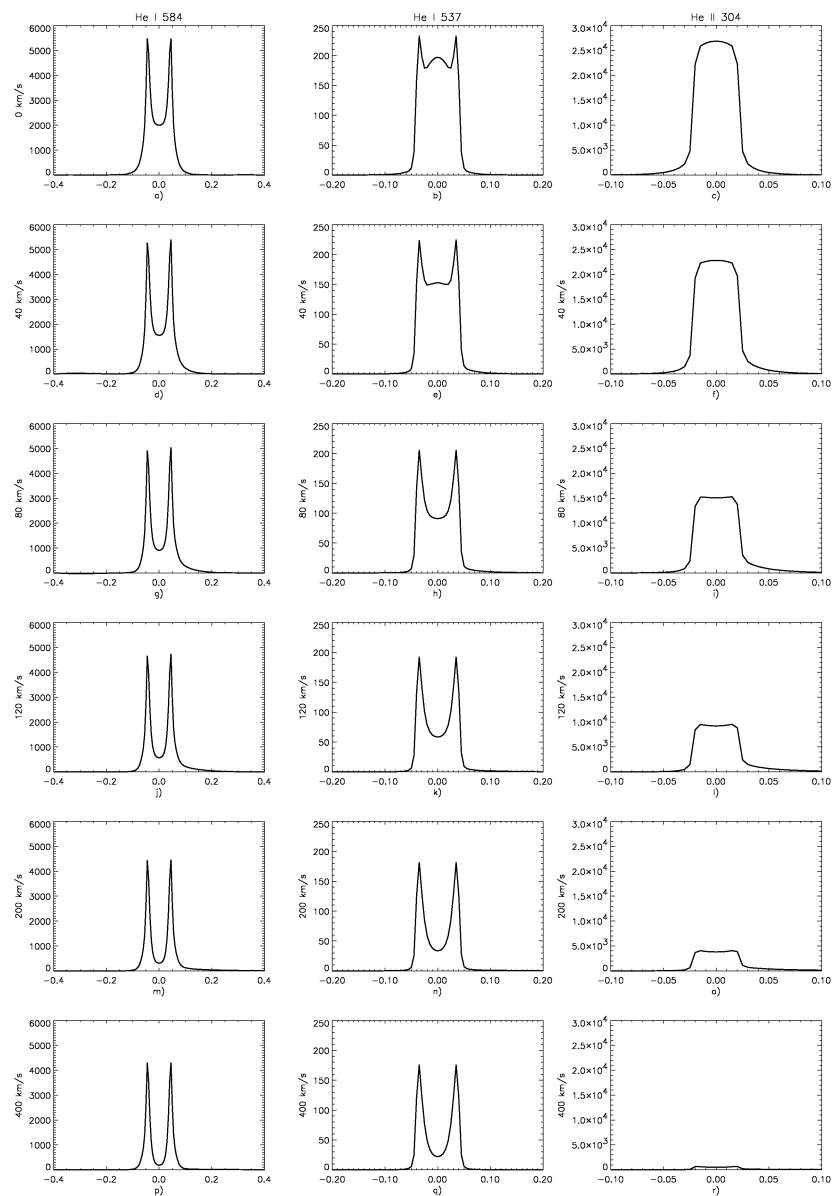


Figure 6. Same as Fig. 5 for  $T=15000$  K.